Research

March 2016

Surveying the Route of a Glacier Outburst Flood (Jökulhlaup) in Western Greenland

rics.org/research

Surveying the Route of a Glacier Outburst Flood (Jökulhlaup) in Western Greenland

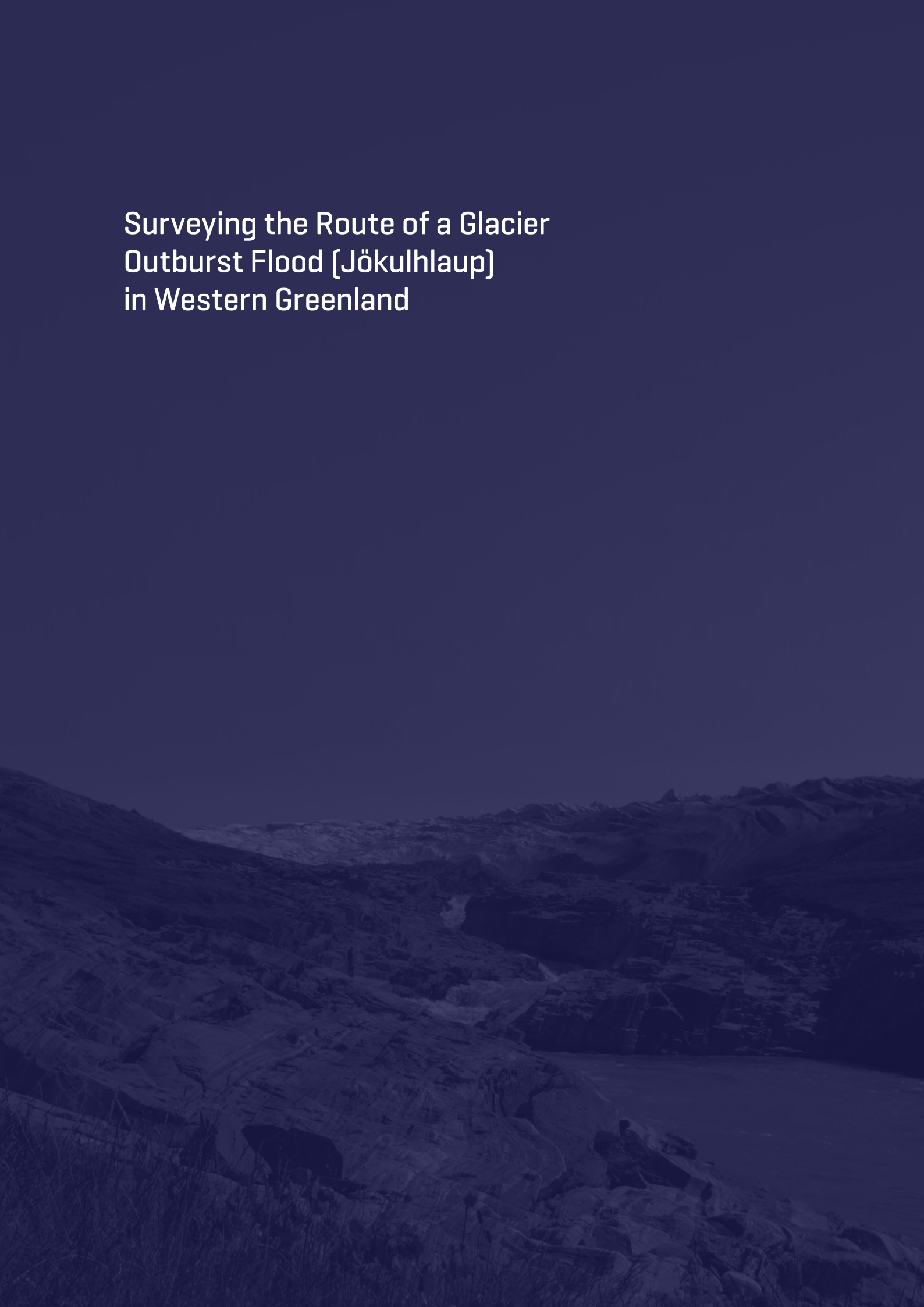

Report for Royal Institution of Chartered Surveyors

Report written by:

Duncan Quincey
Associate Professor in Geomorphology
d.j.quincey@leeds.ac.uk

Jonathan Carrivick
Senior Lecturer in Geomorphology
j.l.carrivick@leeds.ac.uk

Joseph Mallalieu
Research Postgraduate in Geomorphology
j.mallalieu@leeds.ac.uk

RICS Research team

Dr. Clare Eriksson FRICS
Director of Global Research & Policy
ceriksson@rics.org

Amanprit Arnold
Global Research and Policy Manager
aarnold@rics.org

Study sponsored by:

RICS Research Trust

The RICS Research Trust, a registered charity established by RICS in 1955 to support research and education in the field of surveying.

Published by the Royal Institution of Chartered Surveyors (RICS)

RICS, Parliament Square, London SW1P 3AD

www.rics.org

Contents

List of Figures

List of Tables

Glossary

DEM	Digital Elevation Model
GCP	Ground Control Point
GPS	Global Positioning System
Jökulhlaup	Sudden release of water emanating from a glacial source
LiDAR	Airborne laser scanning
SfM	Structure from Motion
UAV	Unmanned Aerial Vehicle

Executive Summary

Background

Glacial lakes can form behind moraine dams (at the glacier terminus) or ice-dams (at the glacier margin), on glaciers themselves, or behind glaciers that advance across main river valleys. Outburst floods from glacial lakes are thought to be increasing in magnitude and frequency in line with a warming climate and ice recession. Currently, ice-dammed lakes are particularly vulnerable to outburst because of the reduction in height and stability of the (melting) dam structure. In many regions, such floods are known as jökulhlaups, a term that originated in Iceland to describe volcanic-glacial floods, but is now used rather more generally to describe any glacier-related outburst. Jökulhlaups can occur without warning, such as when large volumes of meltwater are trapped sub- or en-glacially; others are more predictable, such as when an annual cycle of filling and drainage occurs.

Such floods impact on downstream infrastructure and populations, as well as eroding and depositing volumes of sediment that rapidly advances landscape evolution. Although the geomorphological work carried out by such floods can be crudely quantified across a wide region, relatively little work has been done on the more local scale modification of the flood channel, and in particular how much work is carried out during these extreme events versus 'normal' flows. Studies have been limited by the extreme nature of the events, which preclude in-channel observations, and crude spatial and temporal resolution datasets. These physical processes are thus very poorly represented in flood models, which themselves are normally built upon coarse spatial data, derived from aerial photographs or at best, LiDAR (airborne laser scanning) data, for example.

The technique of Structure from Motion has come to prominence in the geosciences in the last five years, and offers a surveying solution to the coarse-resolution problem. Using theory originally developed to aid in computer vision, it is now possible to create very fine resolution 3D topographic data using imagery acquired by consumer-grade digital cameras, and freely-available open-source software. The resulting point-clouds are comparable in density and in accuracy to those generated by terrestrial laser scanning, and when decimated to 2D data, offer several orders of magnitude more spatial detail than has previously been available. This gives surveyors, scientists and enthusiasts alike the opportunity to study physical processes on the centimetre-decimetre scale, and also to model extreme flood events with much greater accuracy.

The Study

The northern margin of the Russell Glacier, located 35 km east of Kangerlussuaq (Søndre Strømfjord), has been the source of a number of jökulhlaup cycles, dating back to at least the 1940s. Floods have occurred most recently in 2007, 2008, 2010, 2011, 2012 and 2013, all during the months of August or September. Kangerlussuaq is a popular tourist destination, mostly for cruise-ship holidaymakers keen to see, stand on and touch, the world's second largest ice sheet. The region is also home to some exotic Arctic flora and fauna; the musk-ox and the Arctic hare being two species tourists are particularly keen to spot. The tourist industry along this section of the ice-margin is constantly under threat from jökulhlaups originating from the Russell Glacier, and thus makes an excellent natural laboratory to carry out this study, as well as having a very applied focus.

The study was primarily concerned with collecting fine-resolution topographic data with which our hydrological routing (i.e. flood) models could be improved. Current topographic data for the region are derived either from aerial photography (spatial resolution of ~5 m) or, in places, airborne laser scanning (spatial resolution of ~1 m). We thus used the technique of Structure from Motion to derive three new 'reach-scale' digital elevation models, specifically targeted at areas where our previous data were too crude to represent the terrain complexity – i.e. bedrock gorges and waterfalls. We used a combination of hand-held and Unmanned Autonomous Vehicle (UAV) derived imagery to create the 3D models, and georeferenced them using differential GPS ground control data. Further, within each of these three reaches, we used hand-held photography to generate topographic models of fifteen bedrock 'patches' at even finer spatial resolution, to establish baseline topographic datasets with which future surveys can be compared to quantify erosion and deposition during such extreme events.

Key findings

Reach-scale data derived from Structure from Motion can radically improve hydrological modelling

Modelling of three (previously data-crude) parts of the flood channel using the new fine-resolution (0.1 m) topographic models showed great improvement in the detailed simulation of flood extent, water depth, and water velocity. Typically, Structure from Motion (SfM) derived point cloud data comprised 60-90 x 10^6 estimated elevation points with an accuracy of 5-8 cm. When decimated, these data provided 2D digital elevation models comprising > 500000 data points (compared to just 350 data points in previous datasets). This improved detail provides the capability to analyse processes of sediment transfer at much finer scales, as well as providing visualisations of flood flows for public engagement.

Patch-scale models derived from Structure from Motion provides baseline data with which micro-scale erosion and deposition can be quantified

Fifteen topographic models measuring approximately 5 m x 5 m each and comprising 1.16-41.26 x 10^6 points showed detail of individual boulder clusters and subtle hydrological scour features, on a scale of centimetres. Dynamic water surfaces could not be matched between input images and are therefore represented by voids in the cleaned cloud data. Trials using standard deviation metrics (of each cell, once decimated) indicate that leading topographic edges and potential plunge pools, where erosion is likely to be focussed, can be identified using this approach. Quantification of bedrock erosion during the next flood event will thus be possible, providing the first such analysis at this resolution.

Implications for future studies

This research informs surveying, geoscience and natural hazard communities. Surveyors requiring topographic data of the natural environment can use this study as a proof-of-concept and replicate the workflow to generate their own fine-resolution datasets for various applications. Geoscientists may use this tool to study erosion and deposition processes at a scale that has hitherto been impossible, and thus provide the first robust assessment of the geomorphological work carried out during extreme flood flows. This study also provides the natural hazard community with a method to derive much finer detailed predictions of flood flows, to inform disaster preparedness primarily, but also to engage with the general public through flood simulations and visualisations, and to communicate science effectively.

1.0 Introduction

1.1 Background

Outburst floods are sudden releases of water from natural or man-made impoundments. They are recognised as a key landscaping agent on Mars (Baker, 2001), and on Earth include the largest known floods that had important feedbacks with the earth system; affecting thermohaline circulation and exerting widespread and intense landscape change both in terrestrial and continental shelf settings (Baker, 2007). Holocene outburst floods produced bedrock canyons and redistributed vast amounts of sediment across land and into oceans (e.g. Willems et al., 2011). Modern day outburst floods are increasing in frequency and magnitude due to climate change (IPCC, 2014) as warmer air results in (i) increased number and size of meltwater lakes as glaciers diminish (Carrivick and Tweed, 2013; Figure 1), (ii) instability of earth dams due to melting ground ice (e.g. Stoffel and Huggel, 2012), and (iii) failure of landslides damming rivers where the landslide was triggered by permafrost thaw or by pore-water pressurisation and regolith failure due to intense rainfall (Huggel et al., 2012).

Outburst floods are hazardous to people, property and infrastructure. There is no worldwide inventory of socio-economic impacts of outburst floods, but by way of example the 12th May 2008 Wenchuan earthquake caused at least 256 landslides to dam rivers (Chong et al., 2009), which failed producing floods and causing towns and > 200,000 persons to be evacuated. The 16th June 2013 Kedarnath flood caused 4,000 deaths and 100,000 people were airlifted to safety (Sati and Gahalaut, 2013). Outburst flood hazards are persistently highlighted by events in the European Alps (e.g. Keiler et al., 2010), Andes (e.g. Hagan, 2012), Himalaya (e.g. Worni et al., 2013) and Tibet (e.g. Wang et al., 2011), Alaska (e.g. Crossman et al., 2013), Russia (e.g. Petrakov et al., 2012), and Iceland (Bird et al., 2010).

Direct measurements of outburst floods are challenging, so physically-based models often provide the best method for improving our understanding of channel processes and making accurate hazard assessments (Schaub et al., 2013). Such models require topographic information as their fundamental input, and while digital elevation data are now derived routinely from satellite-based and airborne remote sensing sensors, they are at a spatial resolution that cannot represent fine-scale landscape features, and thus produce a crude representation of the flood channel. The technique of Structure from Motion (SfM), which has come to prominence in the last five years, provides another order of magnitude of detail when compared to existing technologies, facilitating the generation of hyperscale landscape models with unlimited temporal frequency and with centimetre point density and accuracy (Brasington et al., 2012; Kerr et al., 2009). It thus has the potential to deliver data that previously have been unavailable through field investigation. By integrating SfM-derived topographic data into physically-based models, there is the potential to create a step-change in the understanding of modern processes and products and of the Holocene record.

Ice-dammed lakes exist in many parts of the world and often pose an extreme hazard when they drain rapidly, producing jökulhlaups (glacial outburst floods).

Figure 1 Examples of different types and stages of ice-marginal lake evolution in Western Greenland.

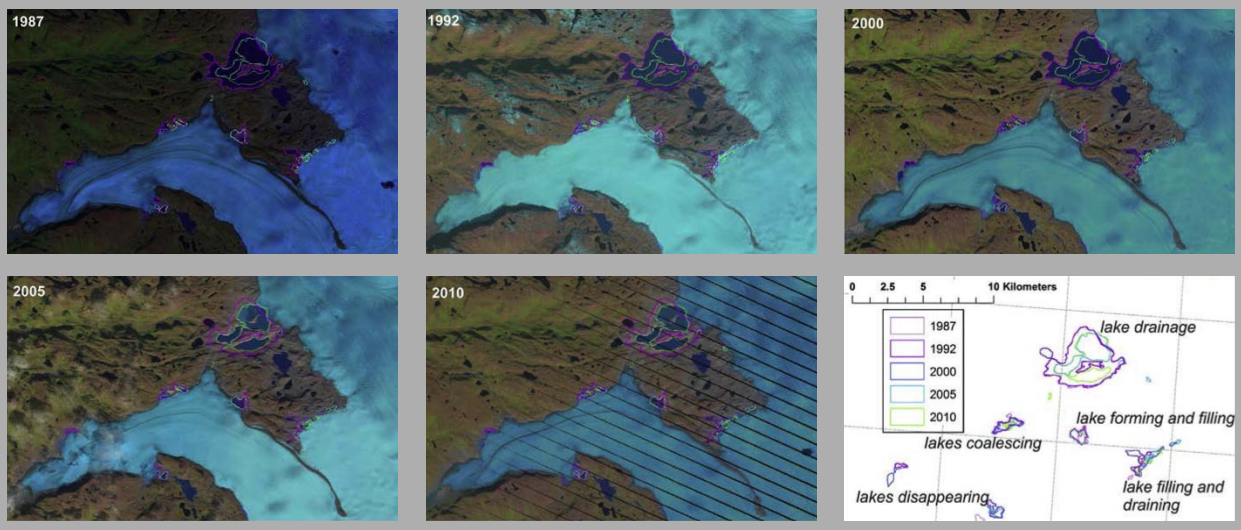

Figure 2 Field photographs of the July 2012 jökulhlaup from the Russell Glacier ice-dammed lake in Western Greenland, the focus of this study.

Images show the damage to property; a 20 tonne mechanical excavator **(a)** and infrastructure; a tourist road **(b)**, as well as the routeway of the flood comprising both expansive valley sandur (outwash plains) **(c)** and bedrock gorges **(d)**.

In western Greenland, some lakes are known to drain periodically, following a cycle that is characterised by 5-10 years of discrete drainage events (Figure 2) followed by long (> 10 years) periods of lake refilling. Although jökulhlaups are initially 100% water by volume and are sediment supply-limited, downstream they are potent agents of rapid landscape change causing erosion of bedrock and entrainment and redistribution of sediment. The bedrock gorges through which flood waters flow have therefore been shaped by a combination of these high-magnitude low-frequency events and 'normal' seasonal flows.

Despite the clear impact these high-magnitude events have on landscape evolution, there are virtually no quantitative data on the geomorphic work carried out by regular meltwater-fed flows vs. extreme flood events. Part of the problem is the inaccessibility of the terrain and the necessity for repeated surveys to detect change, which often rely on traditional methods and can thus be time-consuming and expensive. Another part of the problem is that the available data have not been at sufficient spatial resolution to be able to detect (and therefore model) the erosion and deposition of sediment in flood events. Hydrological models are therefore very poorly constrained in this (quantitative) respect, and since sediment transport is intimately linked to flow hydraulics this limits understanding of outburst flood dynamics, consequent landscape development and hazards posed to life, infrastructure, and property.

1.2 Aims and objectives

The aim of this project was to improve our understanding of outburst floods by capturing an unprecedented set of field data on bedrock channel geometry and erosion during outburst floods. Specifically, we aimed to generate fine-resolution topographic data using Structure from Motion with which future surfaces could be compared, and to extend our existing survey data to those reaches of the routeway that are inaccessible on foot; i.e. bedrock gorges. Both of these new, fine-resolution baseline datasets were to facilitate future calculations of sediment redistribution with unprecedented spatial detail and coverage, thereby permitting better constraint of future channel changes and, ultimately, flood water routing and flow hydraulics.

Our objectives were thus twofold:

1. Derive multiple patch-scale centimetre-resolution digital elevation datasets through fast-flowing (and highly erosive) sections of the flood route using the Structure from Motion surveying technique, to compare with future datasets and quantify sediment movement.
2. Derive multiple reach-scale decimetre-resolution digital elevation models of data-crude sections of the flood route using the Structure from Motion surveying technique to improve modelling and visualisations of extreme flows.

2.0 Site description and previous studies

Our target was an ice-dammed lake situated on the northern margin of Russell Glacier (Figure 3), near Kangerlussuaq (Sondre Stromfjord), western Greenland, which recently started a new jökulhlaup cycle after a 20-year period of inactivity. Drainages occurred on the 31st August 2007, 31st August 2009 and 9th September 2010, and most recently on 10th July 2012. This last event was sourced from extraordinary surface melt rather than a lake outburst, but raised the level of the Watson River, which runs through Kangerlussuaq, west Greenland, to its highest ever recorded level since records began in the 1940s. Historical data indicate several further floods are likely to occur in the jökulhlaup cycle, bringing continued modification of the channel geometry in future years.

Our existing datasets included a range of satellite imagery (Landsat ETM+ (30/06/12), MODIS (08/07/12 to 12/07/12) and ALI (12/07/12) imagery), a 1m grid resolution Digital Elevation Model (DEM) of Sandflugtdalen from NERC ARSF airborne LiDAR data (August 2008), a 5m grid resolution DEM from aerial photogrammetry of Sandflugtdalen and the lower Ørkendalen valleys (August 2006), precise field surveyed river cross-sections obtained with dGPS along the Russell River, water stage measured at the bridge in Kangerlussuaq, and automatic weather station data. We (Russell et al., 2011) previously modelled the exceptional outburst flows that have shaped the flood routeway, and quantified the effect of the channel morphology on these flows (Carrivick et al., 2013). However, very little work to date has been carried out on how outburst flows such as these affect channel morphology, at least on the micro-scale, and this was the gap the current study sought to fill.

Figure 3 **The study area within the context of Western Greenland and detailing the nested lakes through which discharge from the ice-dammed lake drains before entering the flood channel.**

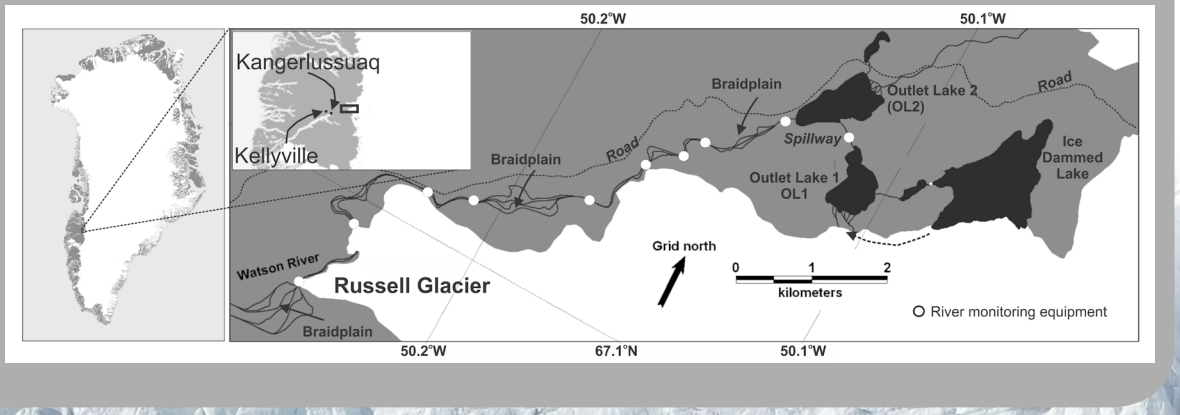

3.0 Research Method

3.1 Topographic surveying

3.1.1 Structure from Motion

Structure from Motion is an image-based method which originated in the discipline of 3D computer vision during the 1980s. It has come to prominence in geological and geomorphological disciplines in the last five years, owing largely to the proliferation of available digital photographic sensors (e.g. in mobile telephones) and airborne platforms (e.g. drones and UAVs) as well as advances in computational power. The method is attractive to surveyors because of the accuracy and the density of the resulting data, which are routinely comparable with those acquired by terrestrial laser scanner (TLS). However, in the case of SfM, the resulting point cloud comprises 3-dimensional coordinates of identifiable features present in the input photographs rather than of pseudo-random points on any surface (as derived by TLS). In addition, because SfM uses visible wavelength photography as its primary input, the resulting point cloud can easily be coloured and interpreted, as opposed to TLS data that are often limited to displaying return intensity or depth. SfM therefore offers several benefits over terrestrial laser scanning, not least in being available for a fraction of the cost.

There are benefits to using SfM over traditional photogrammetric methods too. Although stereo photogrammetry has been successfully used to derive DEM data for many decades, it remains somewhat limited by its rigid input data requirements (usually parallel strips of photos with minimum 60% forward overlap) and the need to specify the camera geometry and acquisition locations as a key part of the workflow. In contrast, SfM is designed to make use of unstructured images that may differ greatly in resolution and scale, and images that are acquired from widely varying locations. SfM algorithms can also handle variations in image brightness and colour, although differences in the direction of illumination can prove problematic where shadows are not common between images used in the model. In contrast to traditional photogrammetry, SfM can calculate camera geometries and positions as part of the feature matching process, although a-priori knowledge of both can improve the accuracy of the resulting model.

Another departure from traditional photogrammetry is the way in which ground control points (GCPs) are used within the process. In traditional photogrammetry GCPs are input before the image 'bundle adjustment' (i.e. the refinement of camera pose and 3D structure) whereas SfM requires the input of GCPs after image matching and the construction of a 3D model. Since GCPs are used as an intrinsic part of the photogrammetric process they can impact on the quality of the final 3D geometry, particularly if they are poor in accuracy themselves or in their distribution across the area of interest. In contrast, SfM data uses GCPs only to reference the point cloud after the 3D scene has been generated, with the many hundreds of image matching points identified as part of the iterative adjustment ensuring the internal (relative) accuracy of the model is robust.

Because of the increasing popularity of SfM, a range of processing software now exists. The workflow commonly follows several major steps. First, homologous 'keypoints' are matched between photographs, for the purpose of reconstructing the basic scene geometry. Secondly, keypoints are refined based on neighbourhood metrics and by identifying inliers and outliers – inliers being only those keypoints that would fit a perfect geometric model. This is an iterative process during which camera orientation of all images, 3D object point coordinates, and camera geometries are adjusted, and results ultimately in the production of a coarse point cloud. Thirdly, object coordinates are resolved for the majority of pixels within the images used in the scene reconstruction, yielding a dense point cloud (comprising one to two orders of magnitude more points than the coarse cloud). Finally, the 3D model is georeferenced, and filtered.

In some respects, the most challenging part of the workflow can be the image acquisition stage (see discussion for recommendations). In Greenland, we collected input imagery by two methods, both of which used a Pentax Q handheld digital camera equipped with a Standard Prime 8.5mm f/1.9 lens to collect the images. For the patch-scale surveys, we circumnavigated each of the patches on foot acquiring between 50 and 70 images at each location, from varying elevations and perspectives. For the reach-scale surveys, we walked on opposite banks acquiring hand-held camera images at every new perspective, and combined them with images acquired from a remotely-controlled unmanned aerial vehicle (UAV) in areas where access was restricted on either bank (Figure 4). Ground control points were marked using water-based (i.e. non-permanent) yellow spray-paint and surveyed using a Leica GPS500 differential GPS with an accuracy of < 1 cm in all cases. In total, we surveyed three gorges at the reach-scale, which were extremely poorly resolved in our existing (LiDAR) survey data, and fifteen patches on exposed bedrock, within the active flood channel (Figure 5).

The images were processed using Agisoft Photoscan Professional and followed a conventional SfM workflow. Images were first roughly aligned to establish initial estimations of camera positions and attitude and to generate sparse point clouds on the order of [103-104] points. We then used a moderate depth filter to derive dense clouds containing 10^6–10^7 points, and cleaned the resulting data by manually removing obvious blunders.

Figure 4 Acquiring aerial imagery from a remotely-controlled UAV for inclusion in Structure from Motion processing.

Figure 5 Overview of the three gorges surveyed at Russell Glacier, west Greenland.

Green dots are ground control points (GCPs), and red triangles are the location of cameras we have monitoring the ice front at the ice-dammed lake; the source of the jökulhlaups in this region. Patch-scale surveys were also located within each of the three gorge sections.

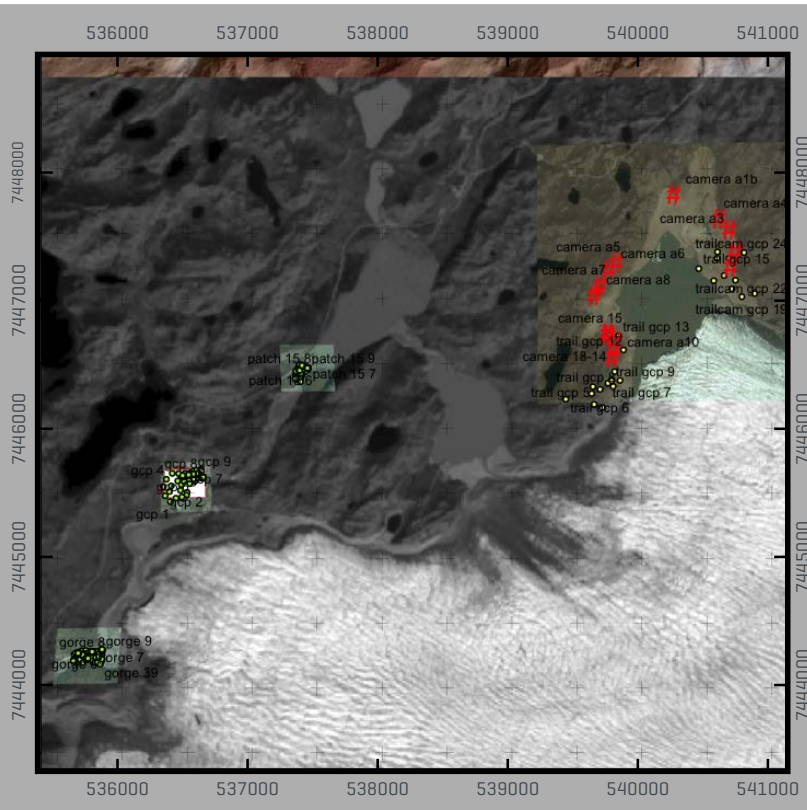

The point clouds were scaled and georeferenced using ground control data acquired in the field (using a Leica GPS500 dGPS; occupation time at each site of 1 minute; typical accuracy of 2-4 cm; Figure 6), then decimated and converted to 2D surfaces using the Topographical Analysis Toolkit (TopCAT; Brasington et al., 2012; Rychkov et al., 2012)[1]. Residual error data (i.e. the difference between source values and the estimated values calculated by PhotoScan) were recorded in each case.

Figure 6 **Typical ground control survey using a Leica GPS500.**

GCPs were marked in soluble yellow marker paint, with a spot (hidden by receiver here) inside a circle acting as the survey point at each location.

3.2 Flood modelling

We used open-source two-dimensional numerical modelling software to simulate extreme flows down each of our three gorge sections. The software is hydrodynamic (i.e. able to fully describe the motion of water) and can incorporate sediment transport and changing bed morphology. It is capable of tracking of a wet/dry front and of capturing shock waves; it accommodates contact discontinuities i.e. steep sediment concentration gradients; it iteratively updates bed elevation; and it can track sediment grain sizes in sequence per grid cell to derive sediment stratigraphy. The need for this model capability is accentuated when such high-resolution DEM data are used, as in this study. The software iteratively accommodates rapidly varying flows to give a water surface and water depth at each input DEM pixel. It is appropriate for this application because: 1. It only depends on an input hydrograph and surface topography, rather than being parameterised by palaeostage indicators that are usually sparse and only describe maximum wash limits (i.e. flood extent); and 2. It can compute transient hydraulic changes through both space and time, which empirical relationships cannot. Here, the initial hydrograph was replicated from data published in Carrivick et al. (2013), derived from the 2008 flood event.

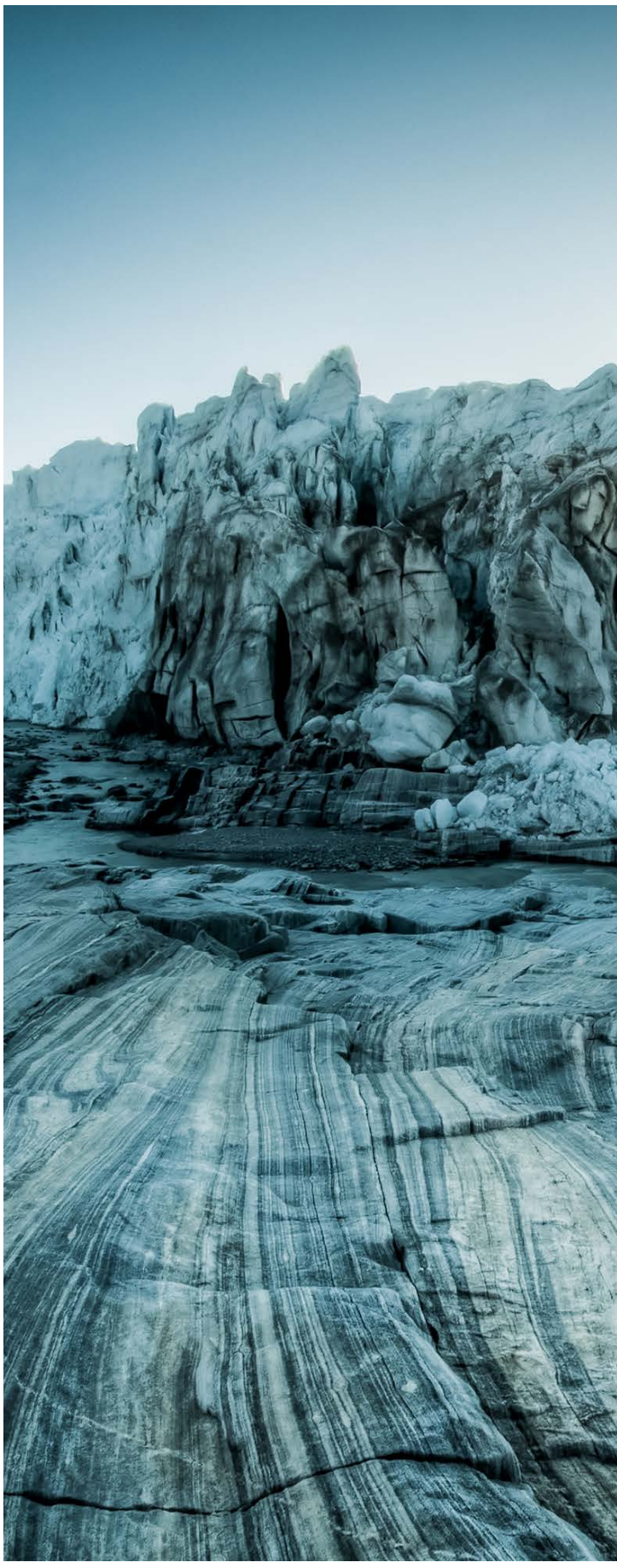

1 This is available for download at http://gcd.joewheaton.org/.

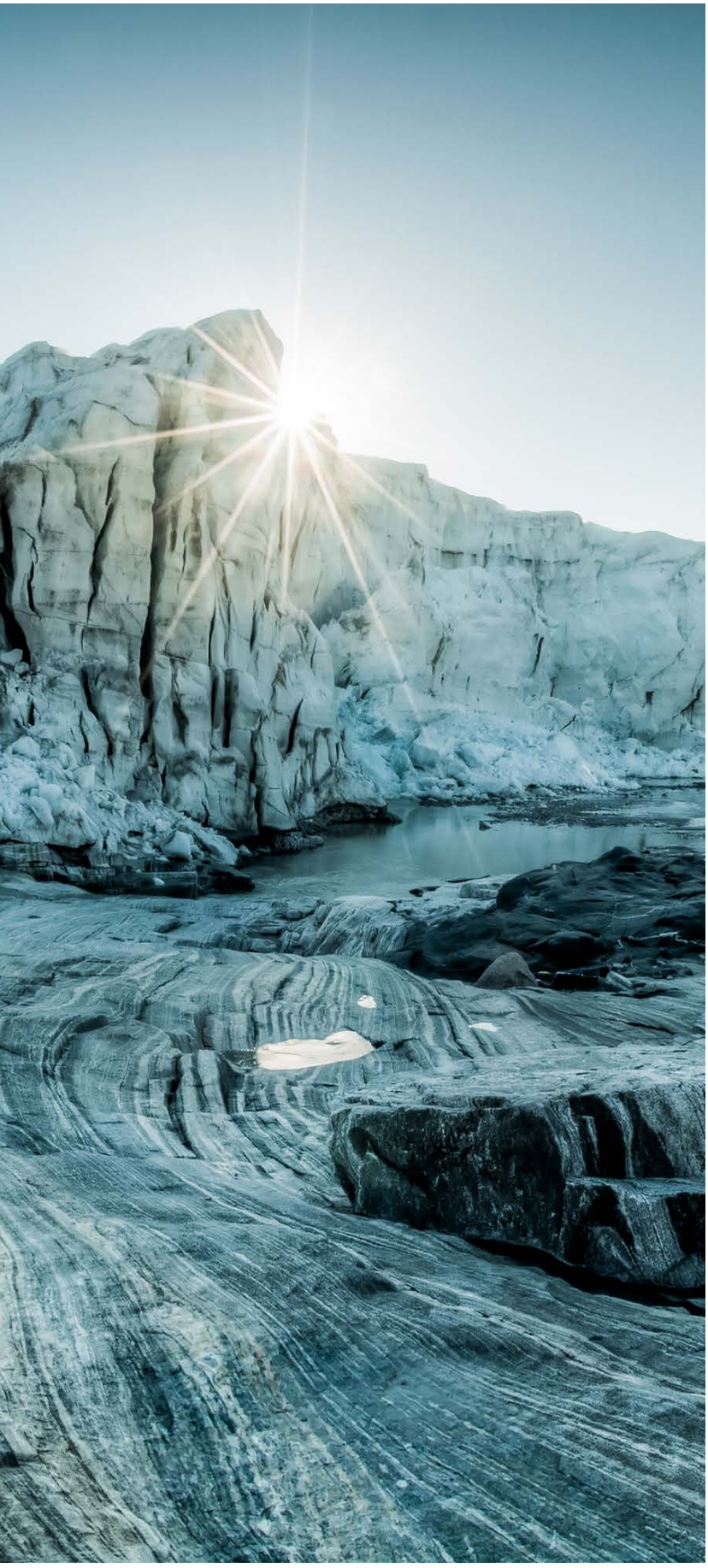

4.0 Results

4.1 Patch-scale surfaces

Fifteen patch-scale surfaces were derived along the Russell Glacier flood route (Figure 7). Point clouds were generated from image sets ranging in size from 44-89 photographs and the total number of points in each cleaned dense cloud ranged from 1.16-41.26 x 10^6. Errors ranged from 0.012-0.031 m. This centimetric accuracy is consistent with reported accuracies for DEMs derived using hand-held consumer-grade sensors and close-range photogrammetry.

Each patch took around one day (eight hours) to process from the initial camera alignment through to presenting a final, filtered and geo-referenced point cloud. Most of the computational time was spent in deriving the dense point cloud (~three hours) and overall computational time was of the order of five hours using a 2.8Ghz Intel Core I5 processor and 2 x 2 Gb of RAM.

Individual point clouds show a remarkable amount of detail (Figure 8; Supplementary Figure S1). It is possible to detect individual boulder clusters (Figure 9) and even relatively subtle hydrological scour features (Figure 10), on a scale of centimetres-decimetres. Although each point cloud comprises > 1 x 10^6 points, there are still areas of no data. These mostly relate to water surfaces (that are dynamic, and thus cannot be matched in non-coincident imagery) and areas of low texture (smooth surfaces such as sand).

Figure 7 **Perspective views of the fifteen patches surveyed along the flood route.**

Numerical data to the right of each patch denotes residual error (reported by Agisoft), the number of points comprising the final point cloud, and the number of images used in processing the patch. For scale, each patch is approximately 5 m across in its longest dimension.

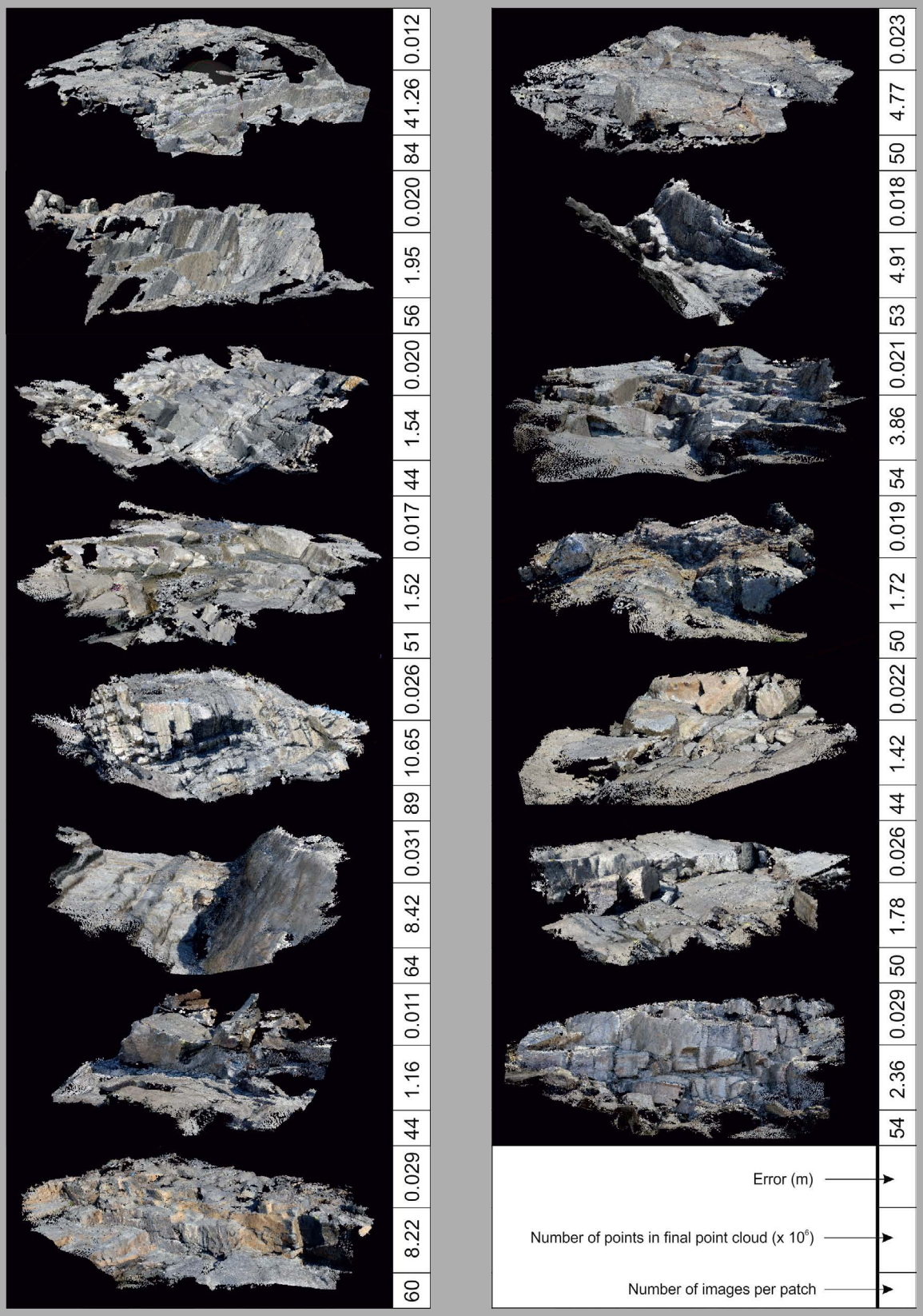

Figure 8 **Patch 3, showing a stepped cascade that is only inundated during extreme flow.**

The leading edges of these stepped flow features, as well as the plunge pools at the base of each step, are likely to be focal points for block detachment and thus erosion. Purple box shows approximate location of Figure 9.

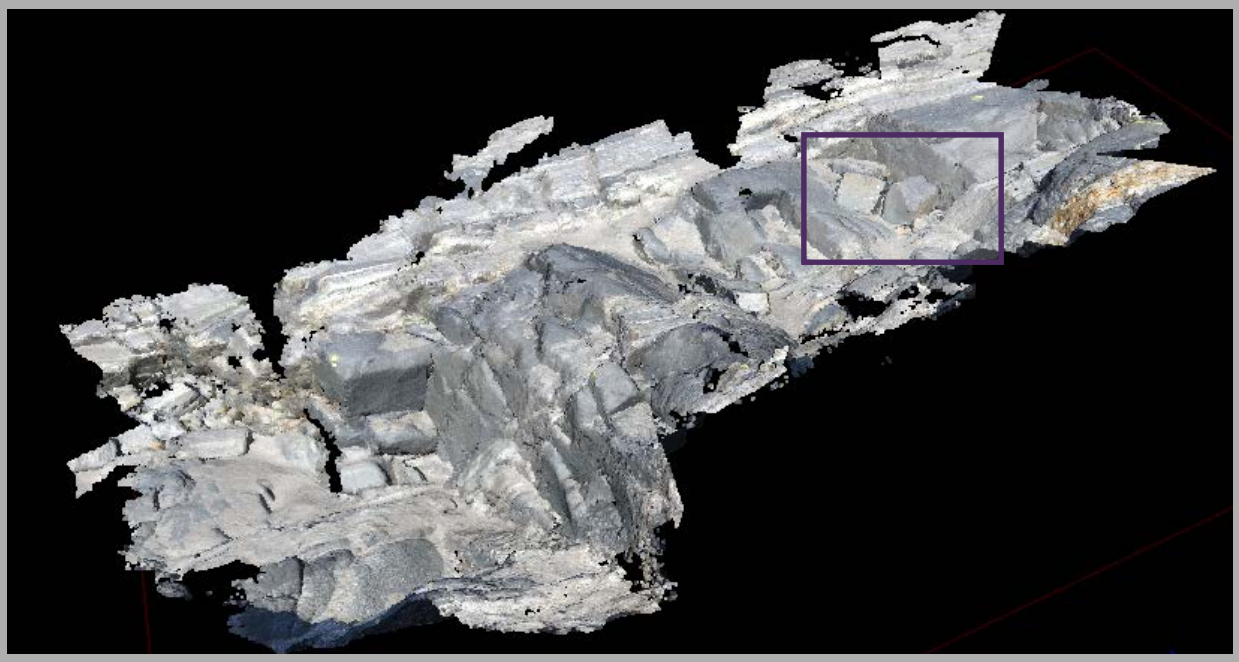

Figure 9 **Subsection of patch 3, as highlighted in Figure 8.**

Detached blocks, presumably deposited by the last major jökulhlaup, rest in the foot of a scoured bedrock step. The height of the step is approximately 0.8 m, for scale.

Figure 10 **Circular scour features (indicated in purple) sculpted by corrasion in areas of concentrated flow.**

4.2 Reach-scale surfaces

Three reach-scale surfaces were derived in areas of poor topographic data in our existing flood route DEM (Figure 11; Table 1). Input image dataset sizes ranged from 203 (patch 3) to 281 (patch 1); cloud sizes were of the order of 70-90 x 10^6 points and the errors ranged from 0.055-0.083 m. Point clouds were decimated to 0.5 m grid resolution DEM data for use in the hydrological modelling. Centimetric accuracy on these new survey data is equivalent to existing LiDAR surveyed sections of the flood route, but exceeds the existing photogrammetrically-derived DEM data accuracy by at least one order of magnitude. These new data also radically improve the level of detail of the three specific reaches; previously Gorge 1, for example, was represented by approximately 350 DEM data points (Figure 11). The decimated 2D SfM dataset comprises 571113 data points.

Each gorge took around 2 days (sixteen hours) of processing time. The largest amount of computational time was spent extracting the dense point clouds (~8 hrs), while overall computational time equated to around thirteen of the sixteen hours. As with the patches, processing was performed using a 2.8Ghz Intel Core I5 processor and 2 x 2 Gb RAM.

The reach-scale point clouds are remarkably dense and show few data voids (Figure 12). The dynamic water surface was manually removed from the final point cloud in each case, since matches in these areas were clear blunders. We used these reach-scale surfaces to improve our modelling of the flood route, by integrating them into an existing Delft3d workflow. The channel was assumed to be parabolic in the absence of any surveyed bed data. Examples of preliminary model runs are depicted in Figure 14, where we match inundation extent corresponding to different discharges to field evidence.

Table 1 **Technical characteristics of the point clouds derived for gorges 1-3**

Gorge number	No. of photos	No. of points (x 10^6)	No. of GCPs	Error (m)
1	281	71.87	37	0.069
2	403	96.78	37	0.083
3	203	68.41	32	0.055

Figure 11 **Detail of gorge one indicating distribution of ground control points for the gorge survey and for each of six bedrock patches.**

The coloured shades denote surface elevation in the final DEM produced by the SfM workflow, the 0.5 m grid resolution of which contrasts with the 5 m grid cell resolution of the best available DEM from photogrammetry as displayed as a grey shade background.

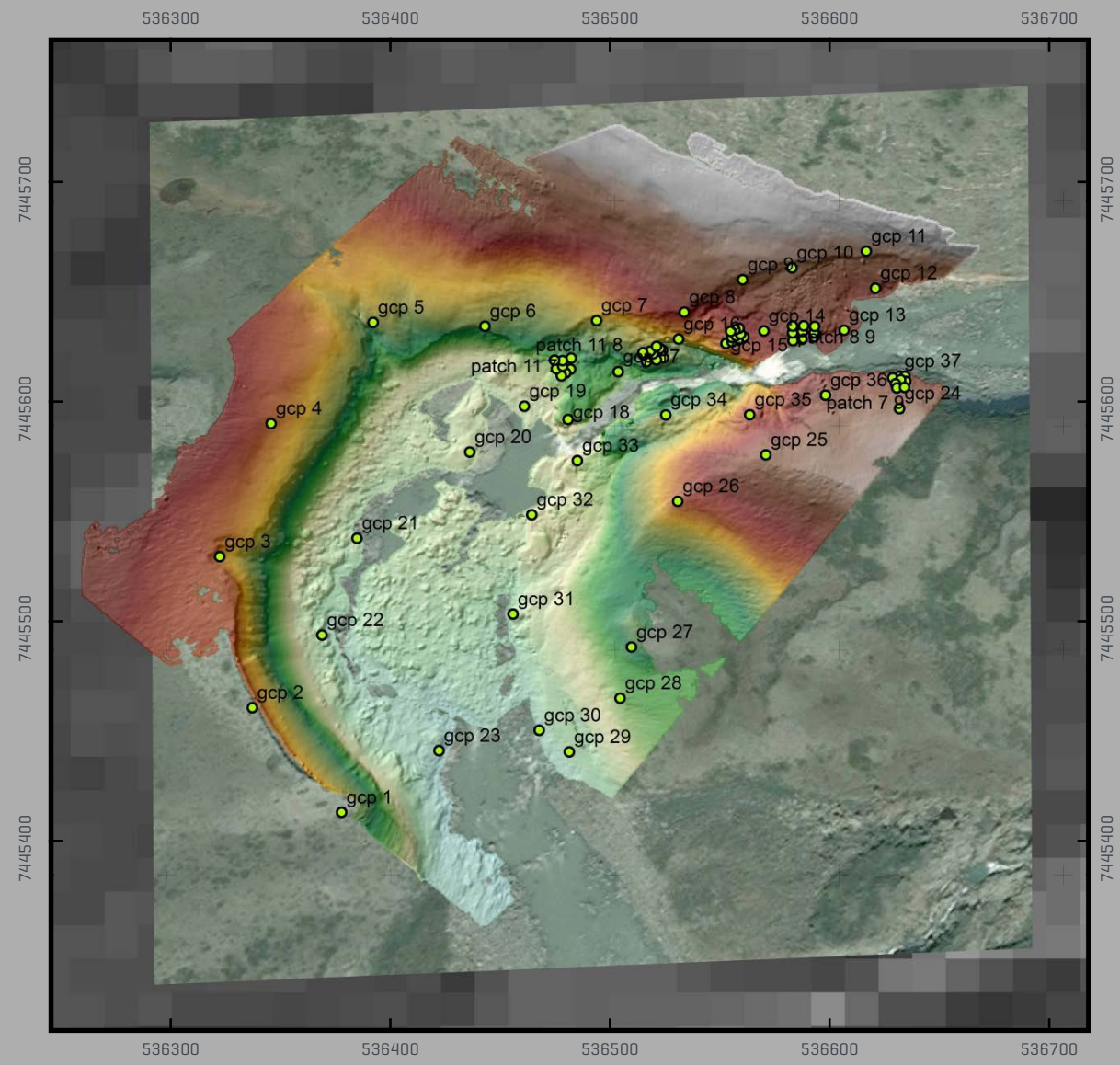

Figure 12 **Gorges 1 (a), 2 (b) and 3 (c), all viewed looking upstream.**

Areas of active channel (i.e. water) are manually removed from these cleaned point clouds; flood limits are clearly visible as the vegetation line on both banks. Yellow arrow in (a) denotes viewpoint depicted in Figure 13.

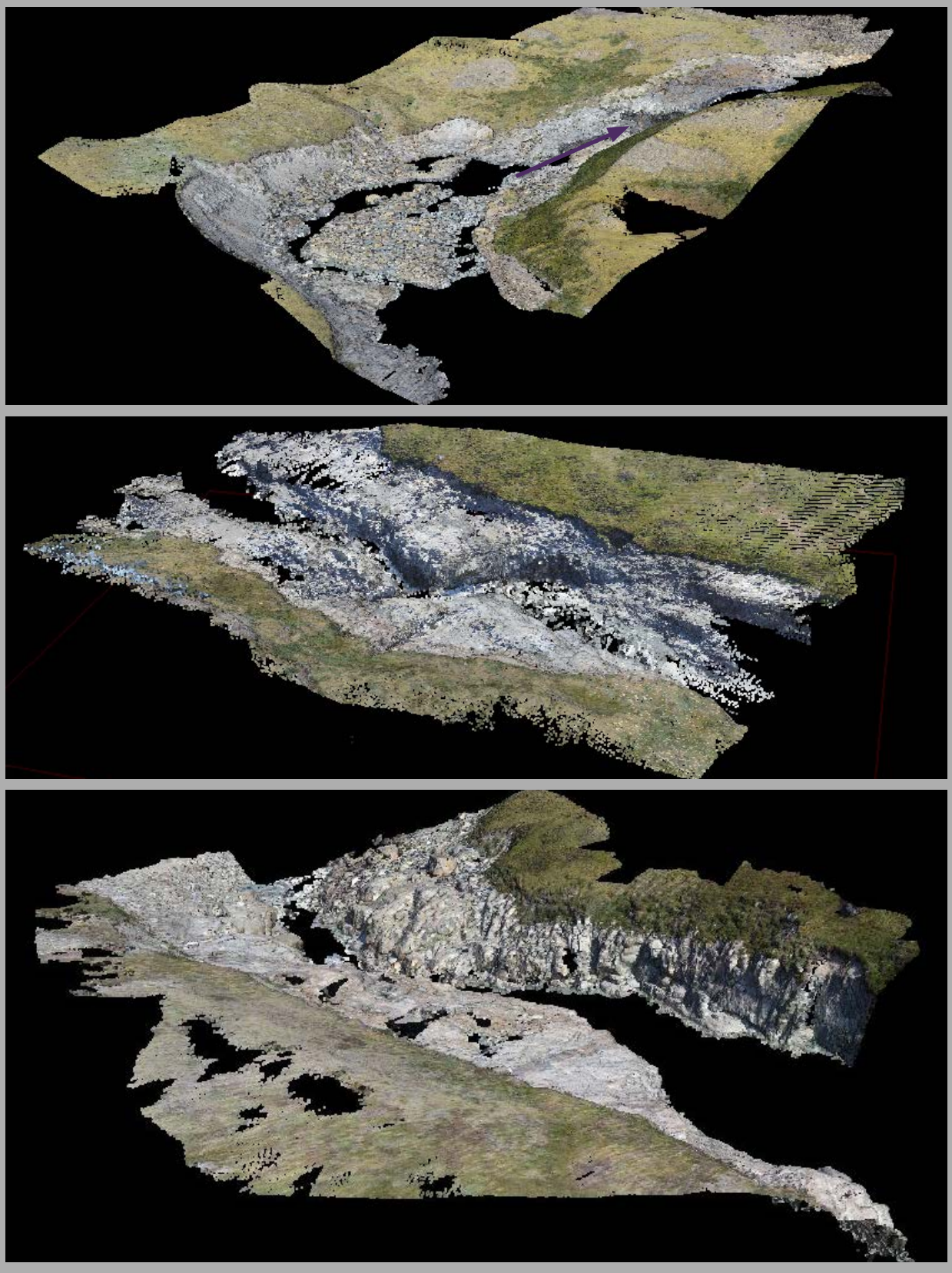

Figure 13 View upstream from centre of flood channel.

The upper reach of this view is a ~10 m high waterfall over which normal flow travels. In times of flood, both banks are inundated, up to the vegetation line at peak flow.

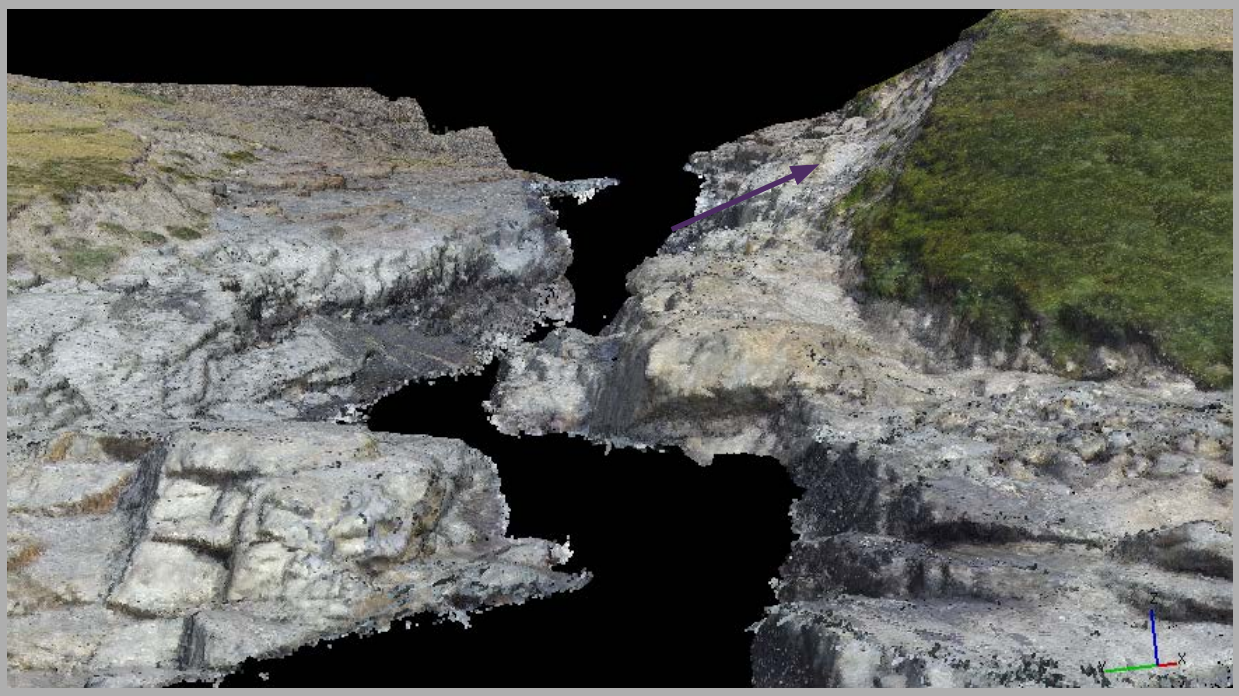

Figure 14 Example of different discharges and resultant inundation extent, water surface and water depth maps.

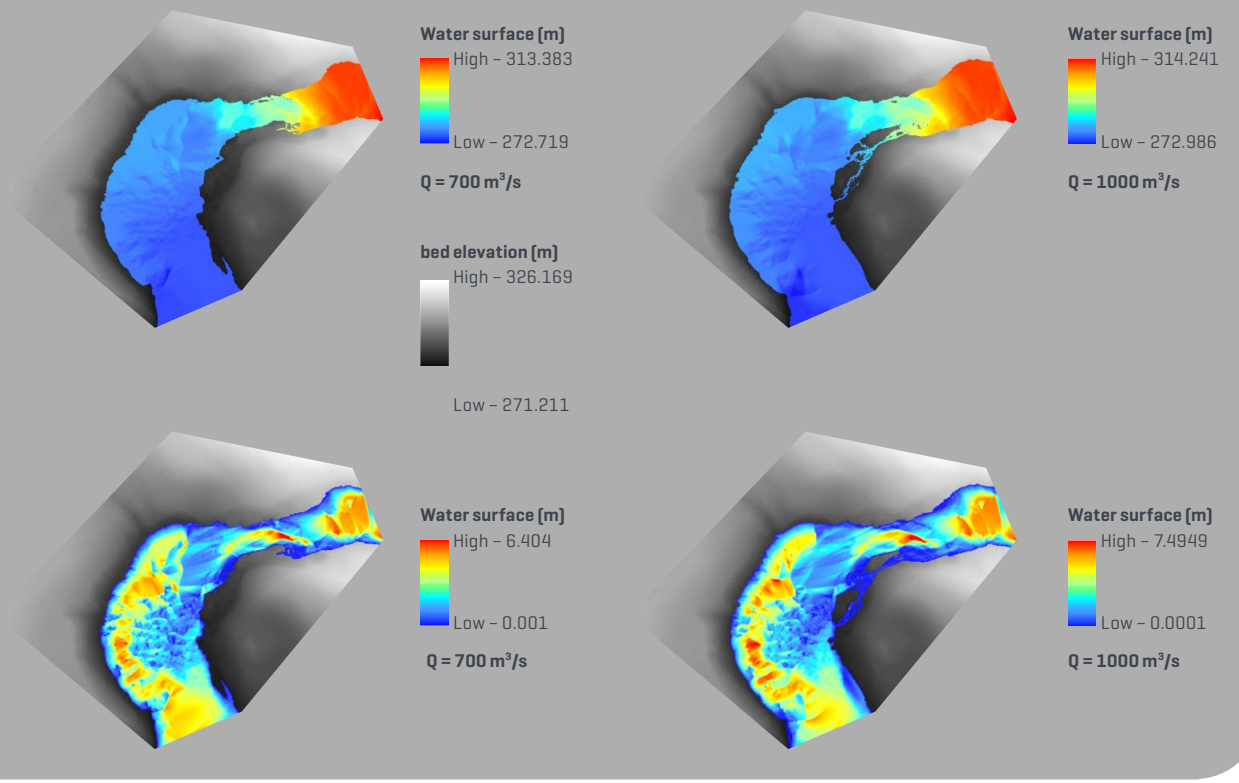

4.3 Visualisations

The photo-realistic point clouds generated by the SfM workflow and the hydraulic modelling when displayed in 3D (Figure 15) are powerful aids to understanding the phenomena and communicating this to stakeholders and the public. In this example it is clear to see how rapid transitions in flow regime can occur, from deep flow to drawn down over a lip to form a near-vertical thin sheet, a waterfall. Immediately beneath the waterfall and within a shallow plunge pool a stopper wave is represented by a discrete zone of super-elevated and deep water. At the foot of the waterfall cascade 'boiling' due to intense upwelling and recirculation is depicted by a hummocky water surface and shallow water depth.

Figure 15 **3D visualisation of floodwater through a ~ 200 m long gorge, as modelled using topography gained from this project using structure from motion (SfM) at 0.5 m grid cell resolution.**

Note the capability of the model to simulate rapidly-varying water surface.

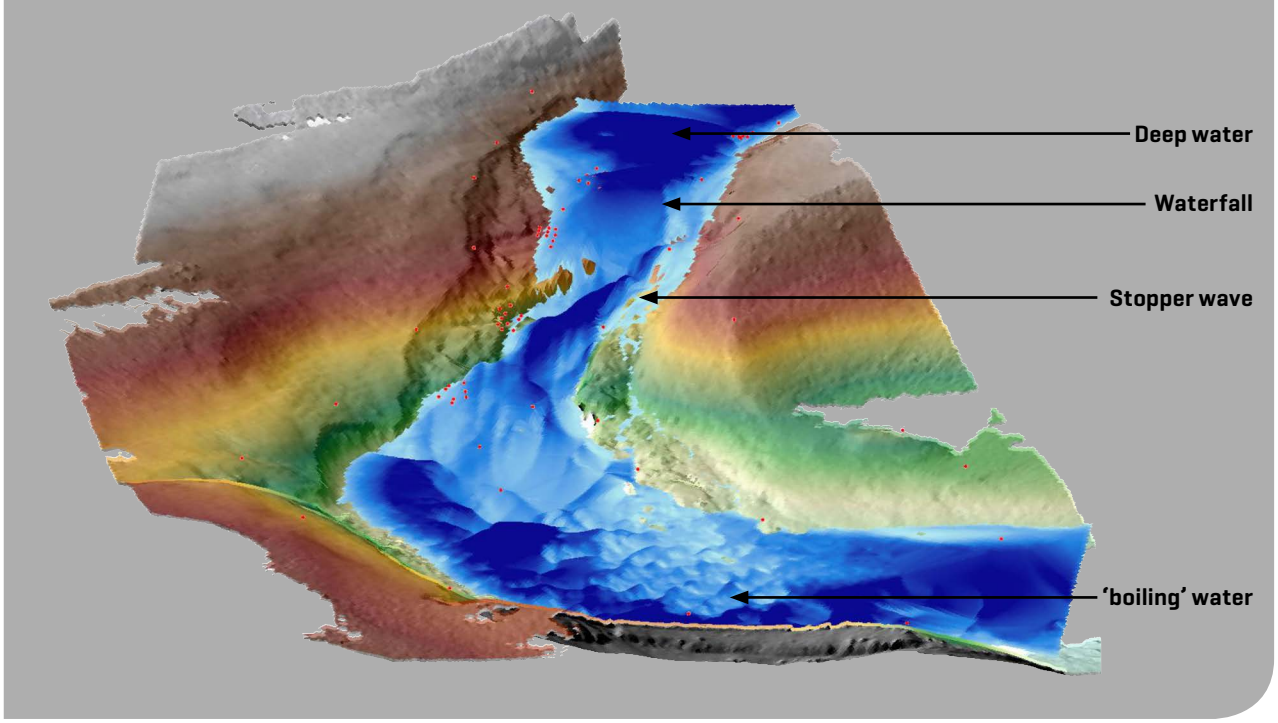

5.0 Discussion

5.1 SfM as a surveying tool

The emergence of SfM promises to be a paradigm shift in surveying methods and is revolutionising the way in which geoscientists collect topographic information. It offers a cost-effective method for surveying outcrops, landforms and other surface properties remotely, quickly, and cheaply, but without compromising on spatial and temporal resolution or data accuracy, both of which are comparable with the currently perceived optimum topographic surveying method (terrestrial laser scanning). Future advances in technology are likely to improve the range of platforms that are available for collecting the required imagery for this method; improve the pixel and radiometric resolution of camera sensors; reduce the required computational time to process large point clouds; and drive down the weight associated with these sensors (making aerial footage easier to acquire).

There are relatively few guidelines available to SfM for how best to acquire imagery for input into the SfM process. Based on our experiences collecting data for this study, we suggest that as a minimum the following 'best practice' should be adopted:

1. Images should be acquired from many different locations rather than many images being acquired from a few locations. The technique depends on the 'motion' aspect of image capture, so the camera should rarely acquire two images from the same/similar position(s).
2. The surveyor should aim to gain 360° coverage of the object or scene of interest.
3. Glare from reflective surfaces and variable contrast across a scene can cause problems for keypoint matching so should be avoided.
4. Textureless scenes (e.g. sand-bars, water surfaces) can also cause problems for keypoint matching so should be avoided.
5. Dynamic surfaces (e.g. moving water) cannot be matched between images, and will require editing once the dense cloud has been extracted. It is therefore sensible to minimise their presence in the acquired images where possible.
6. If a large area of interest is to be surveyed using images acquired over different days, lighting conditions should remain as homogeneous between image sets as is possible. It may, therefore, require the site to be re-visited at the same time each day to minimise contrast and shadow variations.
7. The surveyor should avoid casting their shadow across the scene of interest at all times.

Providing these recommendations are adhered to, and the user has the ability to accurately georeference the resulting point cloud, SfM provides a method that experts and enthusiasts can use in parallel. As algorithms improve (in their ability to identify keypoints from differing standpoints) and sensor pixel resolutions increase, it is inevitable that in some cases the resulting point cloud will massively exceed the point spacing required by the user. In such cases, redundant data can be effectively removed by decimating the point cloud to two-dimensions. Again, based on our experiences here, there are three key issues that the surveyor should be aware of in making the transition from 3D to 2D data:

1. The chosen grid size of the 2D elevation model should be appropriate for the desired application. This involves a trade-off between keeping the model at sufficient resolution to represent the surface topography of interest, but not so fine that it becomes unrealistically computationally expensive.
2. For every order of higher information derived from the original dataset (e.g. calculation of slope and curvature from the DEM data), noise and error will become exaggerated and the effective resolution of the dataset will decrease.
3. Information in the z-axis may be lost and/or modified during processing. This is most critical in areas where several surfaces are represented in the same x,y grid cell – here, converting these multiple elevations into a single elevation point will require some choice of min, max or mean elevation being represented (Figure 16).

5.2 Quantifying erosion and deposition

Bank and bedrock erosion due to outburst floods is rarely measured, very poorly understood and largely ignored in outburst flood models to date. Part of the problem is the inaccessibility of the terrain and the necessity for repeated surveys to detect change, which often rely on traditional point-based surveying methods and can thus be time consuming and expensive to acquire. In contrast, our fifteen patch-scale surfaces were derived at low cost; the major expenses were travel, subsistence and a cheap (< £300) consumer-grade digital camera. In addition, the workflow can be easily replicated following future floods for comparative analyses. This information provides a baseline dataset with which erosion volume and its spatial variability will be quantified following future outburst events, enabling us to take the first step towards integrating these processes into the modelling analysis.

Figure 16 **In this instance, converting the 3D point cloud to a 2D DEM will require some choice of which surface will constitute the final elevation value for the given grid cell.**

Purple arrows indicate choice of surfaces. Conversion of 3D point cloud to 2D planimetric data inevitably loses and/or modifies a large volume of original data, which the surveyor should be aware of.

We anticipate the exact location of erosion will be largely determined by topography; leading edges are more susceptible to bombardment by stones carried in the flood, and also by geological structure. The automatic detection of geological structure from remotely sensed images has been the focus of a number of previous studies, albeit mostly based on satellite or aerial photograph imagery (e.g. Wu and Lee (2007); Argialas and Mavrantza, 2004, Vassilas et al., 2002). Edge detection methods have traditionally focussed on identifying sudden changes in image intensity (e.g. Canny, Sobel, Prewitt, Robert and Laplacian filters); i.e. using image orthophotos rather than digital elevation data. These methods are very effective at demarcating banding and foliation within bedrock surfaces, and also for highlighting fault and fracture surfaces. They are less effective, however, where there is no spectral signature associated with the sudden change in topography.

Patch 2 is an excellent example of this, with the perspective view clearly showing a change in topography, but the orthophoto largely failing to depict this spectrally (Figure 17a and 17b).

In work building on the current study, we therefore intend to focus less on faults and fractures, and more on highlighting topographic edges and potential plunge pool locations – i.e. those where erosive forces will be greatest in extreme flood events. We are thus adopting a novel approach to edge detection, by using the standard deviation of each cell (calculated when decimating the data to two-dimensional DEM data) to automatically detect rapid changes in surface topography (Figure 17d). This method is not affected by image contrast or illumination, factors that can be problematic for existing kernel-based edge detection methods. It is scale dependent however, so we will test the method with DEMs of varying resolution.

Figure 17 Patch 2 in a) perspective view, b) orthophoto, c) decimated to 2D DEM data, and d) with leading topographic edges highlighted using the standard deviation of points within each decimated cell as a proxy for relief.

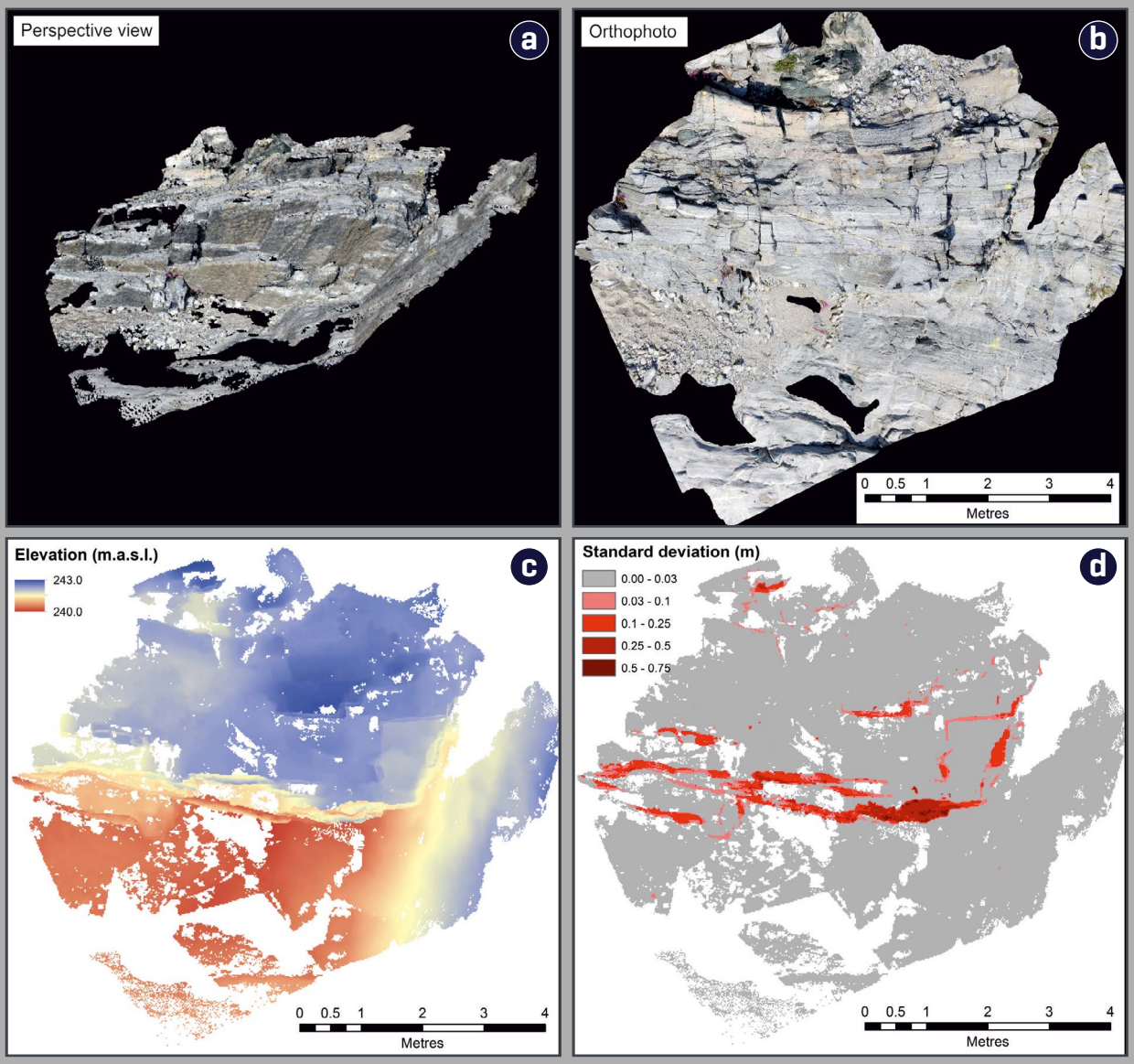

Note there is no spectral change in the orthophoto to depict areas of high and low elevation, as is obvious in the perspective view.

Figure 18 **This modelled jökulhlaup was based on 5 m gridded DEM data and was previously our best estimate of flow velocity and inundation extent for this section of the flood route.**

When compared with Figure 14 above, which shows the same reach, the improvement in detail afforded by the SfM data becomes apparent.

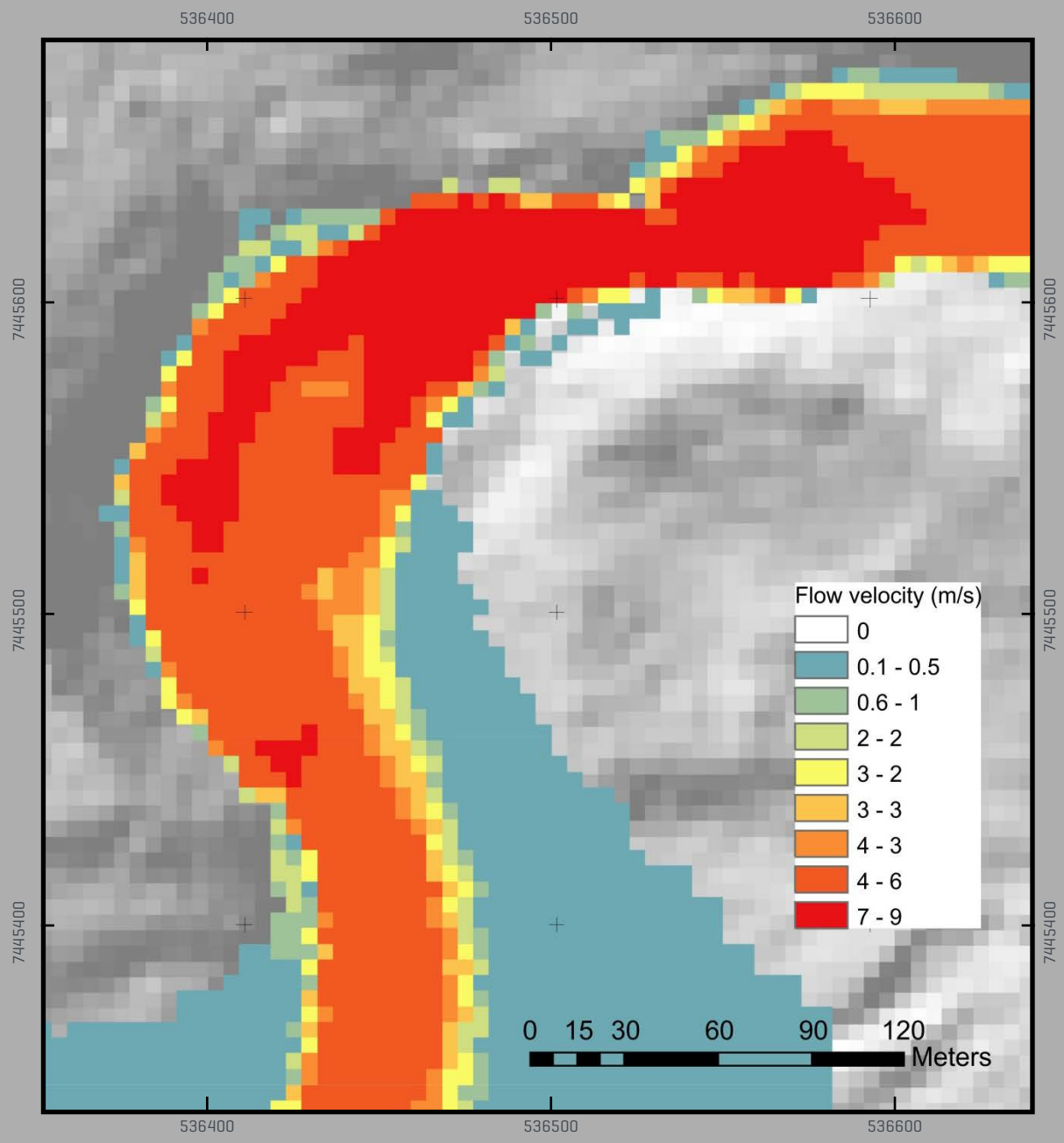

5.3 Improving numerical models

The improvement to the hydrological modelling that the use of a fine-resolution DEM can make becomes apparent when comparing our previous model runs (Figure 18) with those in the current study (Figure 14). From a scientific and hazard management point of view, the ability to model extreme flows in such fine detail is important for two main reasons.

First, it provides the ability to predict areas of inundation with much greater confidence and prepare for sudden floods more effectively. In this research project we demonstrated the benefits of using the finer resolution grid on a relatively sparsely-populated section of the jökulhlaup route, but its true benefit could be realised in simulating extreme flows through the more densely populated town of Kangerlussuaq. Here, the key stakeholders who could benefit from these simulations include the Kangerlussuaq municipality officials responsible for the town's infrastructure and water supply, the airport authorities (because the runway which is the gateway to the whole of west Greenland is bordered by the Watson River), and the local tourism operators. Of course, taking this same approach to modelling outburst floods in more populated areas (e.g. the foothills of the Himalaya) could improve predictions and disaster preparedness even more markedly.

Secondly, given the extra detail afforded by the SfM data, the ability to include sediment transfer processes into the modelling becomes a real possibility. Previous models have neglected or over-simplified sediment transport and thus failed to provide accurate representations of reality. The two field-based studies of Lamb and Fonstad (2010) and Procter et al., (2010) highlighted that sediment entrained in outburst floods: (i) affects the mass and momentum energy of a flow, (ii) results in erosion and deposition which further perturbs flow hydraulics, and furthermore (iii) constitutes a major hazard associated with outburst floods. Lube et al., (2012) demonstrated gain of flood mass due to sediment entrainment and subsequent dilution. Critically, channel geometry changes due to sediment transport have been shown to be both intense and rapid, over 100% in a few minutes (Carrivick et al., 2011), making their inclusion in future numerical simulations a clear challenge for the modelling community.

6.0 Conclusions

The aim of this research was to survey the route of a glacier outburst flood, or jökulhlaup, in western Greenland to i) improve existing hydrological models in areas with crude surface topography data, and ii) to establish a baseline dataset of fine-scale bedrock surfaces with which future surveyed data can be compared.

The aim of the project was fulfilled using SfM, a surveying technique that relies only on images acquired with consumer-grade cameras to generate 3D data of comparable density and accuracy to those derived from terrestrial laser scanning. We surveyed three data-poor reaches of the flood channel, and derived point cloud data comprising > 200 x 10^6 estimated elevation values in total. We also surveyed fifteen bedrock patches, each of which comprised 1-20 x 10^6 estimated elevation values. The former were used to drive a novel computational fluid dynamics (CFD) model that has been designed specifically to represent outburst flood flow characteristics. This was able to show changes in flow regime, the location of plunge pools and areas of upwelling and recirculation in unprecedented detail for this region. The latter will be used to quantify bedrock erosion and deposition following future flood events, enabling the first robust assessment of geomorphological work during a jökulhlaup in this region to be made.

These results invite further investigation into the use of SfM in the geosciences and how it can be used in models of small to medium scale physical processes. The challenge will be to manage ever increasing file sizes as technological improvements permit ever finer resolution data to be generated. Surveyors, geoscientists, practitioners and enthusiasts are all destined to benefit from this paradigm shift in surveying method.

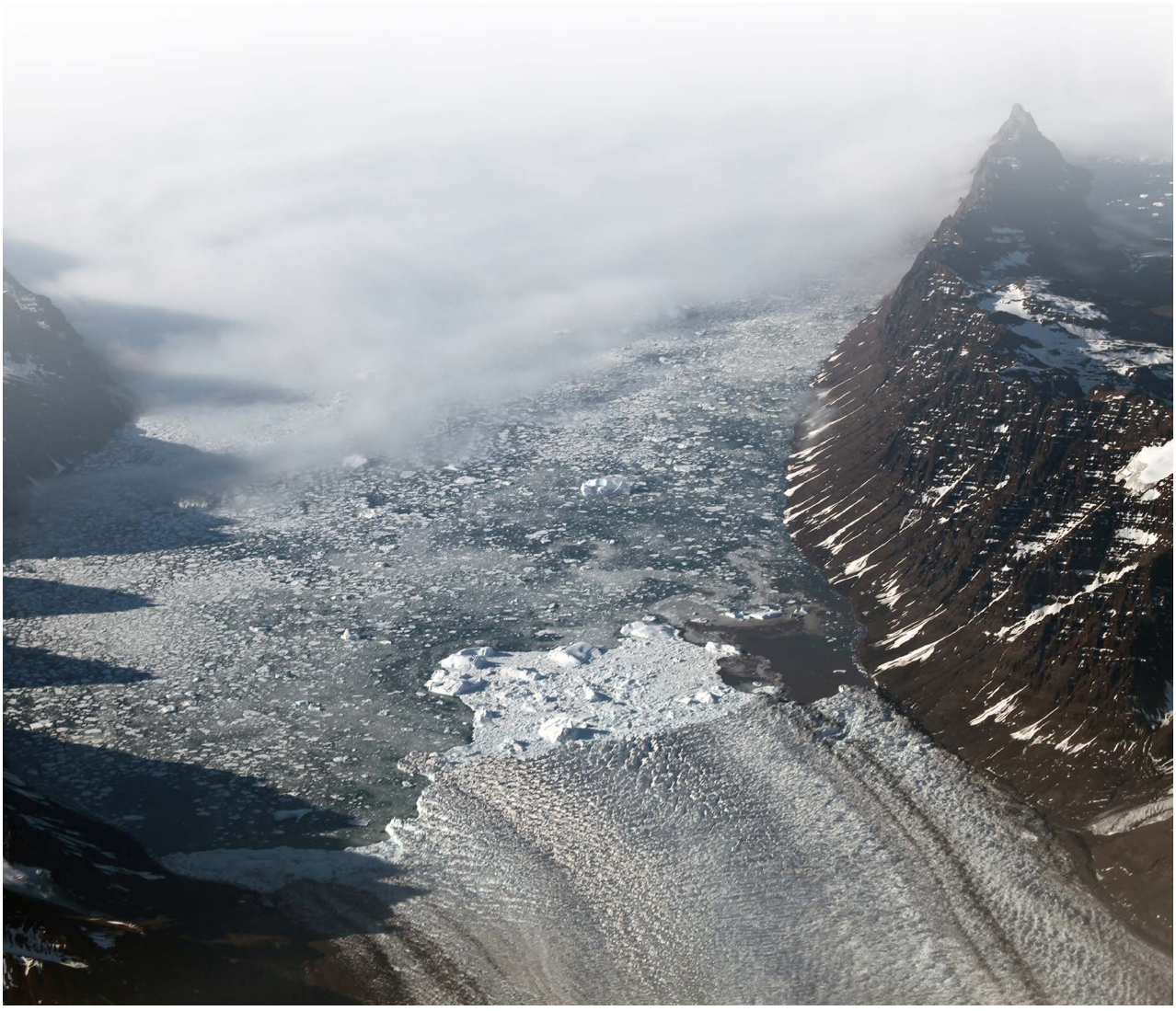

7.0 References

Argialas, D. P., & Mavrantza, O. D. (2004). Comparison of edge detection and hough transform techniques for the extraction of geologic features. International Archives of the Photogrammetry, Remote Sensing and Spatial Information Sciences, 34.

Baker, V. R. (2001). Water and the Martian landscape. Nature, 412(6843), 228-236.

Baker, V. R. (2007). Greatest floods—largest rivers. Large Rivers: Geomorphology and Management, 65-74.

Bird, D. K. (2010). Social dimensions of volcanic hazards, risk and emergency response procedures in southern Iceland.

Brasington, J., Vericat, D., & Rychkov, I. (2012). Modeling river bed morphology, roughness, and surface sedimentology using high resolution terrestrial laser scanning. Water Resources Research, 48(11).

Carrivick, J. L., Jones, R., & Keevil, G. (2011). Experimental insights on geomorphological processes within dam break outburst floods. *Journal of Hydrology*, 408(1), 153-163.

Carrivick, J. L., & Tweed, F. S. (2013). Proglacial lakes: character, behaviour and geological importance. Quaternary Science Reviews, 78, 34-52.

Chong, X. U., Fuchu, D. A. I., & Xin, Y. A. O. (2009). Incidence number and affected area of Wenchuan earthquake-induced landslides. Science & Technology Review, (11), 79-81.

Crossman, J., Bradley, C., Milner, A., & Pinay, G. (2013). Influence of environmental instability of groundwater-fed streams on hyporeic fauna, on a glacial floodplain, Denali National Park, Alaska. River Research and Applications, 29(5), 548-559.

Hagan, N. (2012). In the Shadow of Melting Glaciers: Climate Change and Andean Society. Environmental History, 17(2), 417-419.

Huggel, C., Clague, J. J., & Korup, O. (2012). Is climate change responsible for changing landslide activity in high mountains?. Earth Surface Processes and Landforms, 37(1), 77-91.

IPCC, 2014: Climate Change 2014: Synthesis Report. Contribution of Working Groups I, II and III to the Fifth Assessment Report of the Intergovernmental Panel on Climate Change [Core Writing Team, R.K. Pachauri and L.A. Meyer (eds.)]. IPCC, Geneva, Switzerland, 151 pp.

Keiler, M., Knight, J., & Harrison, S. (2010). Climate change and geomorphological hazards in the eastern European Alps. Philosophical Transactions of the Royal Society A: Mathematical, Physical and Engineering Sciences, 368(1919), 2461-2479.

Kerr, T., Owens, I., Rack, W., & Gardner, R. (2009). Using ground-based laser scanning to monitor surface change on the Rolleston Glacier, New Zealand. Journal of Hydrology (New Zealand), 48(2), 59.

Lamb, M. P., & Fonstad, M. A. (2010). Rapid formation of a modern bedrock canyon by a single flood event. *Nature Geoscience*, 3(7), 477-481.

Lube, G., Cronin, S. J., Manville, V., Procter, J. N., Cole, S. E., & Freundt, A. (2012). Energy growth in laharic mass flows. *Geology*, 40(5), 475-478.

Micklethwaite, S., Turner, D., Vasuki, Y., Kovesi, P., Holden, E. J., and Lucieer, A. (2012). Mapping from an Armchair: Rapid, high-Resolution Mapping using uAV and Computer Vision Technology. Struct. Geol. Resour., 130-133.

Petrakov, D. A., Tutubalina, O. V., Aleinikov, A. A., Chernomorets, S. S., Evans, S. G., Kidyaeva, V. M., Krylenko, I.N., Norin, S.V., Shakhmina, M.S. and Seynova, I. B. (2012). Monitoring of Bashkara Glacier lakes (Central Caucasus, Russia) and modelling of their potential outburst. Natural hazards, 61(3), 1293-1316.

Procter, J., Cronin, S. J., Fuller, I. C., Lube, G., & Manville, V. (2010). Quantifying the geomorphic impacts of a lake-breakout lahar, Mount Ruapehu, New Zealand. Geology, 38(1), 67-70.

Russell, A. J., Carrivick, J. L., Ingeman-Nielsen, T., Yde, J. C., & Williams, M. (2011). A new cycle of jökulhlaups at Russell Glacier, Kangerlussuaq, West Greenland. Journal of Glaciology, 57(202), 238-246.

Rychkov, I., Brasington, J., & Vericat, D. (2012). Computational and methodological aspects of terrestrial surface analysis based on point clouds. Computers & Geosciences, 42, 64-70.

Sati, S. P., & Gahalaut, V. K. (2013). The fury of the floods in the north-west Himalayan region: the Kedarnath tragedy. Geomatics, Natural Hazards and Risk, 4(3), 193-201.

Schaub, Y., Haeberli, W., Huggel, C., Künzler, M., & Bründl, M. (2013). Landslides and new lakes in deglaciating areas: a risk management framework. In Landslide science and practice (pp. 31-38). Springer Berlin Heidelberg.

Stoffel, M., & Huggel, C. (2012). Effects of climate change on mass movements in mountain environments. Progress in Physical Geography, 36(3), 421-439.

Vassilas, N., Perantonis, S., Charou, E., Tsenoglou, T., Stefouli, M., & Varoufakis, S. (2002, April). Delineation of lineaments from satellite data based on efficient neural network and pattern recognition techniques. In 2nd Hellenic Conference on AI, SETN-2002 (pp. 11-12).

Vasuki, Y., Holden, E. J., Kovesi, P., & Micklethwaite, S. (2014). Semi-automatic mapping of geological Structures using UAV-based photogrammetric data: An image analysis approach. Computers & Geosciences, 69, 22-32.

Willems, B. A., Powell, R. D., Cowan, E. A., & Jaeger, J. M. (2011). Glacial outburst flood sediments within Disenchantment Bay, Alaska: implications of recognizing marine jökulhlaup deposits in the stratigraphic record. Marine Geology, 284(1), 1-12.

Worni, R., Huggel, C., & Stoffel, M. (2013). Glacial lakes in the Indian Himalayas—From an area-wide glacial lake inventory to on-site and modeling based risk assessment of critical glacial lakes. Science of the Total Environment, 468, S71-S84.

Wu, T. D., & Lee, M. T. (2007). Geological lineament and shoreline detection in SAR images. In Geoscience and Remote Sensing Symposium, 2007. IGARSS 2007. IEEE International (pp. 520-523). IEEE.

8.0 Acknowledgements

The authors would like to acknowledge:

RICS Research Trust and University of Leeds for financial support; and **Kim Petersen** and **World of Greenland** for providing logistical fieldwork support and **Mingfu Guan** for running the hydraulic model as in figures 14 and 15.

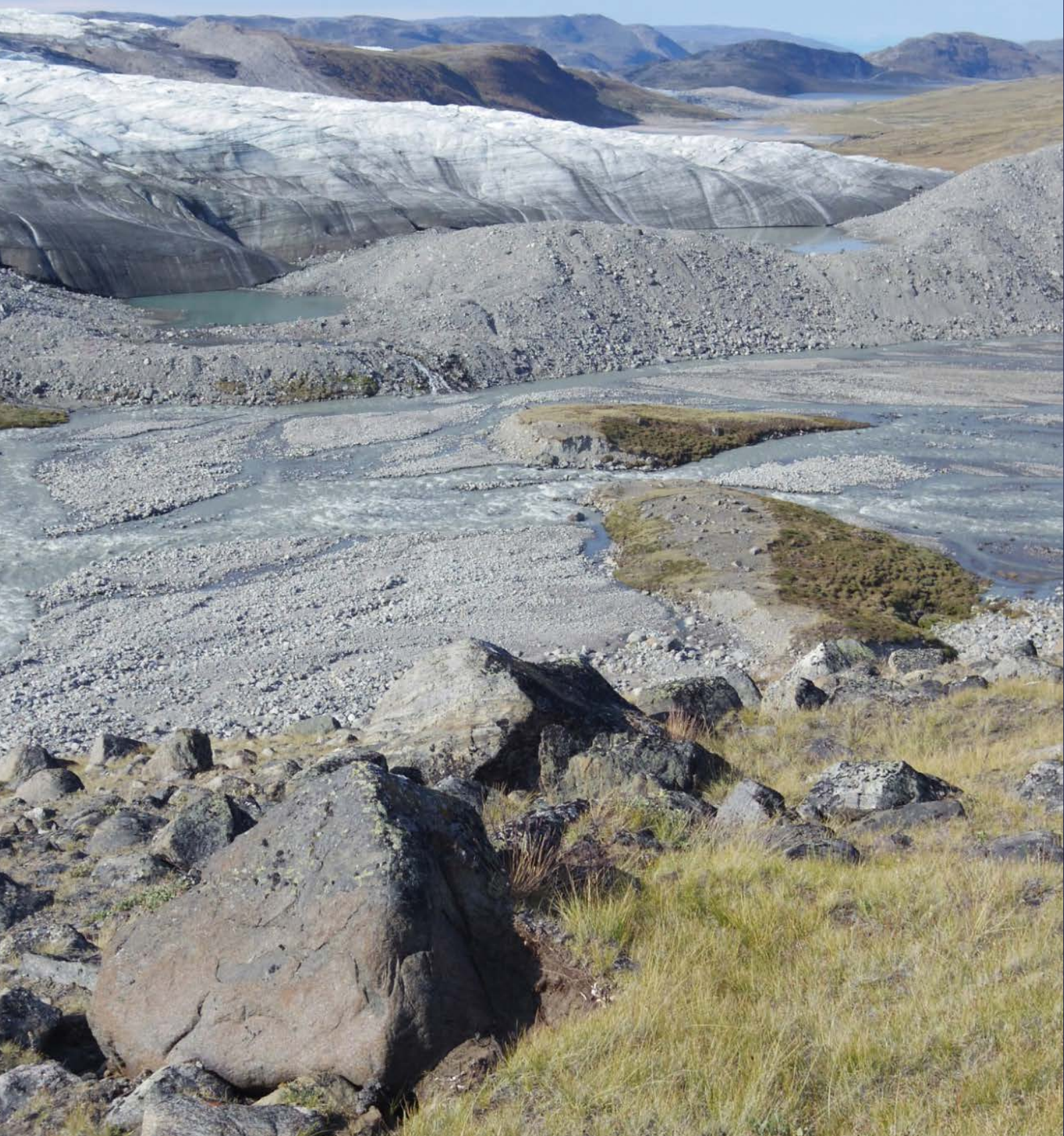

Confidence through professional standards

RICS promotes and enforces the highest professional qualifications and standards in the development and management of land, real estate, construction and infrastructure. Our name promises the consistent delivery of standards – bringing confidence to the markets we serve.

We accredit 118,000 professionals and any individual or firm registered with RICS is subject to our quality assurance. Their expertise covers property, asset valuation and real estate management; the costing and leadership of construction projects; the development of infrastructure; and the management of natural resources, such as mining, farms and woodland. From environmental assessments and building controls to negotiating land rights in an emerging economy; if our members are involved the same professional standards and ethics apply.

We believe that standards underpin effective markets. With up to seventy per cent of the world's wealth bound up in land and real estate, our sector is vital to economic development, helping to support stable, sustainable investment and growth around the globe.

With offices covering the major political and financial centres of the world, our market presence means we are ideally placed to influence policy and embed professional standards. We work at a cross-governmental level, delivering international standards that will support a safe and vibrant marketplace in land, real estate, construction and infrastructure, for the benefit of all.

We are proud of our reputation and we guard it fiercely, so clients who work with an RICS professional can have confidence in the quality and ethics of the services they receive.

United Kingdom RICS HQ
Parliament Square, London
SW1P 3AD United Kingdom

t +44 (0)24 7686 8555
f +44 (0)20 7334 3811
contactrics@rics.org

Media enquiries
pressoffice@rics.org

Ireland
38 Merrion Square, Dublin 2,
Ireland

t +353 1 644 5500
f +353 1 661 1797
ricsireland@rics.org

Europe
(excluding UK and Ireland)

Rue Ducale 67,
1000 Brussels,
Belgium

t +32 2 733 10 19
f +32 2 742 97 48
ricseurope@rics.org

Middle East
Office G14, Block 3,
Knowledge Village,
Dubai, United Arab Emirates

t +971 4 446 2808
f +971 4 427 2498
ricsmenea@rics.org

Africa
PO Box 3400,
Witkoppen 2068,
South Africa

t +27 11 467 2857
f +27 86 514 0655
ricsafrica@rics.org

Americas
One Grand Central Place,
60 East 42nd Street, Suite #542,
New York 10165 – 2811, USA

t +1 212 847 7400
f +1 212 847 7401
ricsamericas@rics.org

South America
Rua Maranhão, 584 – cj 104,
São Paulo – SP, Brasil

t +55 11 2925 0068
ricsbrasil@rics.org

Oceania
Suite 1, Level 9,
1 Castlereagh Street,
Sydney NSW 2000. Australia

t +61 2 9216 2333
f +61 2 9232 5591
info@rics.org

North Asia
3707 Hopewell Centre,
183 Queen's Road East
Wanchai, Hong Kong

t +852 2537 7117
f +852 2537 2756
ricsasia@rics.org

ASEAN
10 Anson Road,
#06-22 International Plaza,
Singapore 079903

t +65 6635 4242
f +65 6635 4244
ricssingapore@rics.org

Japan
Level 14 Hibiya Central Building,
1-2-9 Nishi Shimbashi Minato-Ku,
Tokyo 105-0003, Japan

t +81 3 5532 8813
f +81 3 5532 8814
ricsjapan@rics.org

South Asia
48 & 49 Centrum Plaza,
Sector Road, Sector 53,
Gurgaon – 122002, India

t +91 124 459 5400
f +91 124 459 5402
ricsindia@rics.org

GLOBAL/FEBRUARY 2016/DML/21234/RESEARCH